

High-temperature thermoelectric behavior of lead telluride

M P SINGH¹ and C M BHANDARI²

¹Department of Physics, University of Allahabad, Allahabad 211 002, India

²Indian Institute of Information Technology, Allahabad 211 002, India

E-mail: singhmps74@rediffmail.com; cmbhandari@yahoo.com

MS received 16 November 2003; revised 25 February 2004; accepted 1 April 2004

Abstract. Usefulness of a material in thermoelectric devices is temperature specific. The central problem in thermoelectric material research is the selection of materials with high figure-of-merit in the given temperature range of operation. It is of considerable interest to know the utility range of the material, which is decided by the degrading effect of minority carrier conduction. Lead telluride is among the best-known materials for use in the temperature range 400–900 K. This paper presents a detailed theoretical investigation of the role of minority carriers in degrading the thermoelectric properties of lead telluride and outlines the temperature range for optimal performance.

Keywords. Thermal transport; bipolar conduction; non-parabolicity; figure-of-merits.

PACS Nos 66; 72.10.-d; 72.15.jf; 72.20.pa

1. Introduction

The second half of the twentieth century saw an upsurge of interest in the study of thermoelectric materials [1–6]. With the knowledge that usage of semiconductor thermoelements could result in an enhanced conversion efficiency of a thermoelectric generator, a wide variety of semiconductors were investigated. As a result three thermoelectric technologies were identified in the early stages of thermoelectric material research: silicon–germanium alloys for high-temperature applications ($T > 1000$ K) [7–12], lead telluride and other chalcogenides [13–23] for the intermediate temperature range (400–1000 K), and bismuth telluride-based materials [24–28] for lower temperatures ($T < 400$ K).

Applicability of a thermoelectric device (generator or refrigerator) is temperature specific. For every potential thermoelectric material, a utility range can be identified beyond which its usefulness is questionable. This kind of study is centered around the role played by the minority carriers (holes in n-type, electrons in p-type semiconductor) in degrading the material performance. The degrading influence may come through the minority contribution to Seebeck coefficient, or electrical

and thermal conductivities. Recently Gurevich *et al* [29] have presented a detailed theoretical study of thermoelectric effects in bipolar semiconductors. Their work takes into account the non-equilibrium distribution of electron and hole concentrations.

The paper presents a brief account of the role of minority carriers in thermoelectric studies and their effectiveness in defining the utility range of thermoelements based on lead telluride. The device performance is determined by the so-called thermoelectric figure-of-merit $Z = \alpha^2\sigma/\lambda$, where α , σ and λ refer to the Seebeck coefficient, electrical conductivity and thermal conductivity, respectively, of the material under study.

2. Theory

A parabolic band model usually provides a good description of electron (hole) energy bands. This simplification arises from the inclusion of only first term of a more general expansion of electron energy $E(k)$ about the band edge. Higher order terms in the expansion are hard to neglect at higher carrier densities, particularly in narrow gap semiconductors. Parabolic approximation can be reasonably valid when electron (hole) states near the conduction (valence) band edge are occupied. As the bands get more populated, electron behavior at the top of the band cannot be described in the usual manner. The carrier effective mass is no more a constant and shows a dependence on carrier energy and energy band gap.

Transport coefficients for such a situation can be obtained by adopting an approach in which electron energy is described by [13,14,30]

$$\frac{\hbar^2}{2} \frac{2k_T^2}{m_{T0}^*} + \frac{\hbar^2}{2} \frac{k_L^2}{m_{L0}^*} = E \left(1 + \frac{E}{E_g} \right). \quad (1)$$

Here k_L and k_T refer to longitudinal and transverse components of the electron wave vector, m_{L0}^* and m_{T0}^* are the longitudinal and transverse components of the effective mass tensor at the band edge, E refers to the carrier energy measured from the band edge and E_g is the energy band gap. The energy dependence of the effective mass is given by $m_{P0}^* (1 + 2\eta\beta_g)$ where $P = L$ or T , for transverse and longitudinal components. For non-parabolic energy bands the transport coefficients are usually expressed in terms of the generalized Fermi integrals defined by [31]

$${}^n L_l^m(\xi, \beta_g) = \int_0^\infty \left(-\frac{\partial f}{\partial \eta} \right) \eta^n [\eta (1 + \beta_g \eta)]^m (1 + 2\beta_g \eta)^l d\eta. \quad (2)$$

Here f refers to Fermi distribution function, $\xi = E_F/k_B T$ is the reduced Fermi energy, $\eta = E/k_B T$ is the reduced carrier energy and $\beta_g = k_B T/E_g$ is the inverse of the reduced energy band gap, respectively.

2.1 Electron scattering processes

Electronic transport depends on the carrier density and mobility which itself depends upon the mean free path lengths between successive collisions. Transport

coefficients are derived from Boltzmann equation in the framework of relaxation time approximation. In a pure and perfect crystal, the carriers are primarily scattered by the thermal vibrations of the crystal lattice. Both the acoustic and the optical phonon modes shall be considered in the temperature range of interest. The relaxation times for electron scattering by acoustic and optic modes are given by [31]

$$\tau_{\text{ac}} = \frac{2\pi\hbar^4 C_{11} E^{-1/2}}{k_B T \varepsilon_1^2 (2m^*)^{3/2}}, \quad (3)$$

$$\tau_{\text{po}} = \frac{\hbar^2 E^{1/2}}{e^2 k_B T (2m^*)^{1/2} (\varepsilon_\infty^{-1} - \varepsilon_0^{-1})}. \quad (4)$$

Here C_{11} is the elastic constant, ε_1 is the deformation potential constant, ε_∞ and ε_0 are the high frequency and static dielectric constants.

The expressions for Seebeck coefficient and dimensionless Lorenz number L_f , which is defined as $(\lambda_e/\sigma T) = (k_B/e)^2 L_f$ where λ_e is the electronic contribution to thermal conductivity and σ is the electrical conductivity (for acoustic phonon scattering and polar optical phonon scattering), are given by [18,21,31]

$$\alpha_{\text{ac}} = \frac{k_B}{e} \left(\xi - \frac{{}^1L_{-2}^1}{{}^0L_{-2}^1} \right), \quad \alpha_{\text{po}} = \frac{k_B}{e} \left(\xi - \frac{{}^1L_{-2}^2}{{}^0L_{-2}^2} \right),$$

$$L_f^{\text{ac}} = \frac{{}^2L_{-2}^1}{{}^0L_{-2}^1} - \left(\frac{{}^1L_{-2}^1}{{}^0L_{-2}^1} \right)^2, \quad L_f^{\text{po}} = \frac{{}^2L_{-2}^2}{{}^0L_{-2}^2} - \left(\frac{{}^1L_{-2}^2}{{}^0L_{-2}^2} \right)^2. \quad (5)$$

2.2 Two-band model

A single band (conduction or valence) provides a reasonably good description of transport mechanism for high carrier densities and relatively lower temperatures. However, for low carrier densities and relatively higher temperatures, contributions from both the bands may become comparable and use of a two-band model is essential. With both bands contributing to electric current, total electrical conductivity [5,32] is $\sigma = \sigma_e + \sigma_h$ and Seebeck coefficient for the two-band model is given by [5]

$$\alpha = \left[\frac{\alpha_e \sigma_e + \alpha_h \sigma_h}{\sigma_e + \sigma_h} \right], \quad (6)$$

where subscripts e and h refer to contributions from electron and hole bands.

2.3 Thermal conductivity

The thermal conductivity of a semiconductor is mainly due to the lattice contribution. However, semiconducting materials are heavily doped, and hence both the

electronic and hole contributions may become significant. In the range of intrinsic conduction the bipolar contribution to thermal conductivity λ_b should also be taken into consideration [5,31]. The total thermal conductivity can be written as $\lambda = \lambda_L + \lambda_e + \lambda_h + \lambda_b$ where the bipolar contribution λ_b is given by [5]

$$\lambda_b = T \left(\frac{k_B}{e} \right)^2 \frac{\sigma_e \sigma_h}{\sigma_e + \sigma_h} [\delta_e + \delta_h + \xi_g]^2. \quad (7)$$

The subscripts L, e, h, and b refer to lattice, electron, hole and bipolar contributions, respectively and $\delta_{e,h} = ({}^1L_{-2}^1/{}^0L_{-2}^1)_{e,h}$ for acoustical phonon scattering and $\delta_{e,h} = ({}^1L_{-2}^2/{}^0L_{-2}^2)_{e,h}$ for optical phonon scattering.

2.4 Figure-of-merit

For a single-band model (the conduction band or the valence band) the dimensionless thermoelectric figure-of-merit is given by [18,32]

$$(ZT)_{SB} = \frac{(\alpha'_n)^2 \sigma'_n}{1 + L_{fn}^{ac} \sigma'_n}, \quad (8)$$

where α'_n refers to reduced Seebeck coefficient and defined by $\alpha'_n = (e/k_B)\alpha_n$, σ'_n refers to the reduced electrical conductivity and defined by $\sigma'_n = (k_B/e)^2(T/\lambda_L)\sigma_n$, and dimensionless Lorentz number $L_{fn}^{ac} = ({}^2L_{-2}^1/{}^0L_{-2}^1) - ({}^1L_{-2}^1/{}^0L_{-2}^1)^2$. The suffix n is replaced by e and h for contributions from electron and hole bands. However, as temperature increases a significant population of electrons may be excited across the energy gap and intrinsic conduction may become appreciable. As a result the effect of both the bands has to be taken into consideration. The dimensionless figure-of-merit for a two-band model is given by [5,18]

$$(ZT)_{2B} = \frac{(\alpha'_h \sigma'_h - \alpha'_e \sigma'_e)^2}{[(\sigma'_e + \sigma'_h) (1 + \sigma'_e L_{fe}^{ac} + \sigma'_h L_{fh}^{ac})]}, \quad (9)$$

where

$$\alpha'_{e,h} = \frac{e}{k_B} \alpha_{e,h}, \quad \sigma'_{e,h} = \left(\frac{k_B}{e} \right)^2 \frac{T}{k_L} \sigma_{e,h}.$$

When electron and hole number densities are comparable, electron-hole pairs diffuse down the temperature gradient, thereby carrying heat but no charge. Referred to as bipolar thermal conductivity, its inclusion modifies the figure-of-merit which is now given by [5,18]

$$(ZT)_{ac} = \frac{(\alpha'_h \sigma'_h - \alpha'_e \sigma'_e)^2}{[(\sigma'_e + \sigma'_h) (1 + \sigma'_e L_{fe}^{ac} + \sigma'_h L_{fh}^{ac}) + \sigma'_e \sigma'_h (\delta_e + \delta_h + \xi_g)^2]}. \quad (10)$$

Similar expression can be written down for optical phonon scattering. When more than one electron (hole) scattering mechanisms are appreciable, ZT can be obtained separately for the two cases. The combined effect of the two calculations on ZT can be approximately described by [5,23]

$$\frac{1}{ZT} = \frac{1}{(ZT)_{ac}} + \frac{1}{(ZT)_{po}}. \quad (11)$$

3. Results and discussion

The theoretical formulation described above has been applied to obtain the thermoelectric figure-of-merit of lead telluride. Physical parameters required in the calculation [33] are displayed in table 1. Theoretical expressions of electronic and thermoelectric coefficients are usually expressed in terms of the reduced Fermi level (ξ), and in all calculations this is treated as a variable spanning a range of values from non-degenerate limit to the degenerate limit. Theoretical procedure requires transport coefficients to be calculated for a given electron scattering mechanism. If there are more than one scattering mechanism operating simultaneously, the electronic properties under consideration may be obtained separately for each scattering mechanism. For lead telluride thermoelements, the most useful operating temperature range is 400–900 K. Hence the present study focusses attention in this particular range. The two dominant carrier scattering mechanisms – scattering by acoustic phonons and by optical phonons have been considered.

Figure 1 displays thermoelectric figure-of-merit ZT against reduced Fermi level ξ at 650 K for acoustic phonon scattering for parabolic and non-parabolic nature of energy bands. The choice of $T = 650$ K is based on the fact that ZT shows a maximum between 600 and 700 K when plotted against temperature. It is apparent from the results that band non-parabolicity has a significant effect on the thermoelectric performance of lead telluride and that exclusion of non-parabolicity overestimates ZT for optimally doped samples by around 30–40%. Figure 2 shows ZT against ξ at 650 K for acoustic phonon scattering, optical phonon scattering and both taken together in accordance with eq. (11). Figure 3 shows ZT against T for different values of ξ in the region of optimal doping. Also shown are the experimental results of two different samples taken from literature [34,35].

A number of conclusions can be drawn from the present studies. These are:

- (a) A two-band conduction model is essential for the entire range of doping except in very heavily doped materials. At 650 K, $(ZT)_{max}$ for single-band

Table 1. Physical parameters of PbTe at 300 K used in the calculation.

C_{11} (10^{11} N m ⁻²)	m^*/m_0	λ_L (W m ⁻¹ K ⁻¹)	E_g (eV)	Nv^a	ϵ^b (eV)	ϵ_0^c	ϵ_{00}^d
1.39	0.2	1.7	0.32	4	24	400	38

^aNumber of equivalent valleys. ^bAcoustic deformation potentials.

^cStatic dielectric constant. ^dHigh-frequency dielectric constant.

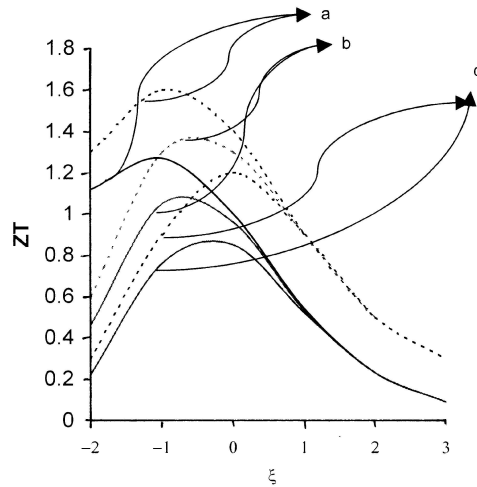


Figure 1. Variation of dimensionless figure-of-merit ZT with reduced Fermi energy ξ at $T = 650$ K for single band model (curves a), two-band model without bipolar thermal conduction (curves b) and bipolar contribution included (curves c). The solid line refers to a non-parabolic band, dashed line refers to a parabolic band.

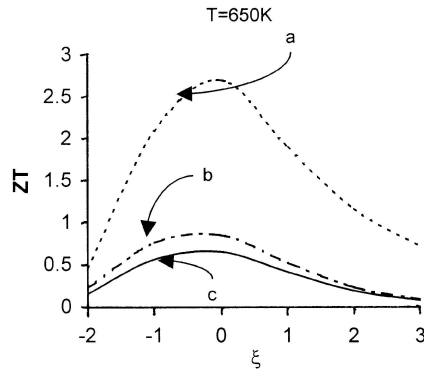


Figure 2. Variation of ZT with reduced Fermi energy ξ at $T = 650$ K for polar optical scattering (curve a), acoustic scattering (curve b), and both scattering combined (curve c).

model and two-band model without and with bipolar contribution to thermal conductivity (λ_b) are 1.25, 1.06, and 0.83, respectively.

- (b) The effect of non-parabolicity is significant in the entire range of Fermi levels considered. Any calculation of electronic properties of lead telluride must therefore take into account the non-parabolicity of the energy bands.
- (c) Acoustic phonon scattering is the dominant scattering in limiting the electronic mean free path. However, optical phonons have significant effect on the electronic properties. $(ZT)_{\max}$ at 650 K for acoustic phonon scattering

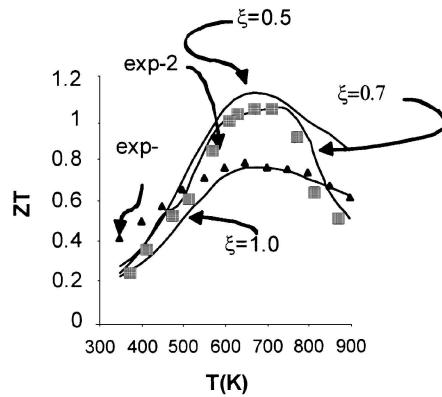


Figure 3. Variation of ZT with temperature at $\xi = 0.5$, $\xi = 0.7$ and $\xi = 1.0$. Experimental values reported in literature [34,35] are also shown in the figure.

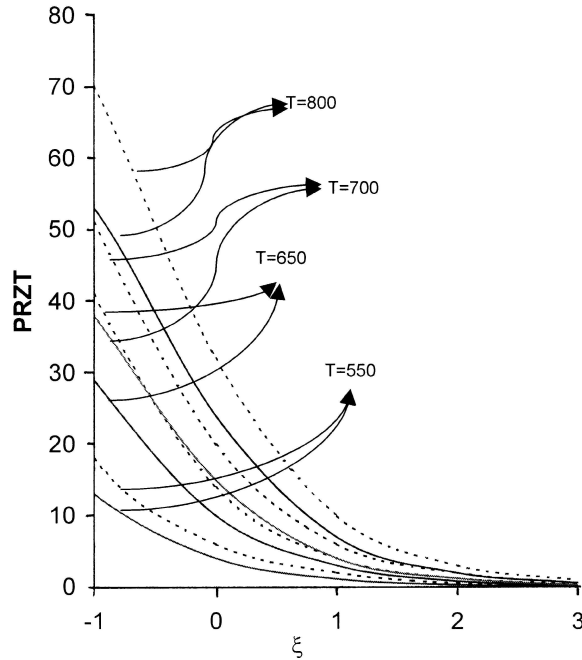


Figure 4. Percentage reduction in ZT (PRZT due to MCE (dashed line) and MCE(B) (solid line)) plotted against reduced Fermi energy ξ at $T = 550, 650, 700$ and 800 K.

is 0.8 and for both scattering mechanisms is 0.65. Neglecting optical phonon scattering would cause an error of around 22% in overestimating ZT .

Thermoelectric devices are temperature specific and thermoelectric performance is degraded with the onset of minority carrier effects. Presence of minority carriers

influences the properties in two ways: (a) Seebeck coefficient and electrical conductivity contributions from the other band and (b) bipolar thermal conduction. We refer to all minority effects included as MCE and only bipolar thermal conductivity as MCE(B). Figure 4 shows the minority carrier contribution in reducing ZT , over the corresponding single-band values, and defined by $\text{PRZT} = \frac{\Delta Z}{Z} \times 100$, plotted against ξ . These results bring out some more details about the thermoelectric performance of lead telluride. These are:

- (1) Maximum in ZT occurs at around 650–700 K for various ξ values.
- (2) At 650 K, $\xi_{\text{opt}} \cong -0.5$ which refers to $n \cong 8 \times 10^{24} \text{ m}^{-3}$. In general, the most useful optimal doping range is 3×10^{24} – 10^{25} m^{-3} .
- (3) At 650 K effectiveness of MCE in reducing ZT from single-band values is around 40% and at 750 K this goes up to 70% for $\xi = -1$.
- (4) Bipolar thermal transport, which is usually ignored in minority carrier effects, has a significant role in influencing the thermoelectric properties and performance. At 650 K the bipolar term alone changes ZT by around 20% whereas total change with both MCE included may be around 30%.
- (5) Most useful temperature range of operation for PbTe thermoelements is 500–800 K.

Acknowledgement

M P Singh thankfully acknowledges financial assistance from the Council of Scientific and Industrial Research, New Delhi, India. Authors thank Prof. G K Pandey and Dr. M D Tiwari for their interest and support.

References

- [1] A F Ioffe, *Semiconductor thermoelements and thermoelectric cooling* (Infosearch, London, 1957)
- [2] I B Cadoff and J Miller, *Thermoelectric materials and devices* (Reinhold, New York, 1958)
- [3] H J Goldsmid, *Applications of thermoelectricity* (Methuen Monograph, London, 1960)
- [4] P H Egli (ed.), *Thermoelectricity* (John Wiley and Sons, New York, 1960)
- [5] D M Rowe and C M Bhandari, *Modern thermoelectrics* (Holt-Saunders Ltd, London, 1983)
- [6] H J Goldsmid, *Electronic refrigeration* (Pion Ltd, London, 1968)
- [7] V Raag, *Proc. 10th Intersociety Energy Conversion Engg. Conf.* (IEEE, New York, 1975) p. 156
- [8] C M Bhandari and D M Rowe, *Contemp. Phys.* **21**, 219 (1980)
- [9] D M Rowe, *J. Power Sources* **19**, 247 (1987)
- [10] G A Slack and M Hussain, *J. Appl. Phys.* **70**, 2694 (1991)
- [11] C Vining and J R Fleurial, *Proc. 10th International Conf. on Thermoelectrics* edited by D M Rowe (Cardiff, 1991) (Babrow Press, Wales, U K)
- [12] M N Tripathi and C M Bhandari, *J. Phys.* **C15**, 5359 (2003)
- [13] Yu I Ravich, B A Efimova and V I Tamarchenko, *Phys. Status Solidi* **B43**, 11 (1971)

High-temperature thermoelectric behavior of lead telluride

- [14] Yu I Ravich, B A Efimova and V I Tamarchenko, *Phys. Status Solidi*. **B43**, 453 (1971)
- [15] Yu I Ravich, I A Smirnov and V V Tikhonov, *Sov. Phys. Semicond.* **1(2)**, 163 (1967)
- [16] C M Bhandari and D M Rowe, *J. Phys.* **D16**, L75 (1983)
- [17] C M Bhandari and D M Rowe, *Appl. Phys. Lett.* **47**, 256 (1985)
- [18] D M Rowe and C M Bhandari, *Sixth Int. Conf. on Thermoelectric Energy Conversion* (Arlington, 1986) p. 186
- [19] G Nimtz and B Schlicht, *Narrow-gap Lead Salts*, Springer Tract in Modern Physics, *Narrow-gap semiconductors* edited by G Hohler (Springer, Berlin, 1983) Vol. 98
- [20] T C Herman, D L Spears and M P Walsh, *J. Electron. Mater.* **28(1)**, L1 (1999)
- [21] C M Bhandari and D M Rowe, *First European Conference on Thermoelectrics* edited by D M Rowe (1987) p. 178
- [22] Yu I Ravich, B A Efimova and I A Smirnov, *Semiconducting lead chalcogenides* (Plenum, New York, 1970)
- [23] S A Nemov and Yu I Ravich, *Sov. Phys. Usp.* **41(8)**, 735 (1998)
- [24] R S Ainsworth and W W Scanlon, *Phys. Rev.* **111**, 1029 (1958)
- [25] J P Fleurial, T Y Rocca Serra, H Scherrer and S Scherrer, *First European Conf. on Thermoelectrics* (Cardiff, 1987)
- [26] H Scherrer and S Scherrer, *Handbook of thermoelectrics* edited by D M Rowe (CRC Press, New York, 1994)
- [27] M Stordeur, *Handbook of thermoelectrics* edited by D M Rowe (CRC Press, New York, 1995)
- [28] G S Nola, J Sharp and H J Goldsmid, *Thermoelectrics – Basic principles and new materials development* (Springer Verlag, 2001)
- [29] Yu G Gurevich, O Yu Titov, G N Longvinov and O I Lyubimov *Phys. Rev.* **B51**, 6999 (1995)
- [30] E O Kane, *J. Phys. Chem. Solids* **1**, 249 (1957)
- [31] C M Bhandari and D M Rowe, *Thermal conduction in semiconductors* (Wiley Eastern Limited, New Delhi, 1988)
- [32] C M Bhandari, in *Handbook of thermoelectrics* edited by D M Rowe (CRC Press, New York, 1995) Chapters 4–6
- [33] C M Bhandari and D M Rowe, *Proc. Ninth European Conference on Thermophysical Properties* edited by Roy Taylor (Pion Limited, Manchester, UK, September 1984)
- [34] Yu I Ravich, in *Handbook of thermoelectrics* edited by D M Rowe (CRC Press, New York, 1995) Chapter 7
- [35] D M Rowe, *Marine Technol. Soc. J.* **27(3)**, 43 (1997)